Journal of Geosciences and Geomatics, 2015, Vol. 3, No. 4, 96-108
Available online at http://pubs.sciepub.com/jgg/3/4/2

DOI:10.12691/jgg-3-4-2

Mineral Alteration and Chlorite Geothermometry in Platinum Group Element (PGE)- Bearing Meta-ultramafic Rocks from South East Cameroon

Ako T. A.[1,2,*], A. Vishiti[1,3], K. I. Ateh[1], A. C. Kedia[1], C. E. Suh[1]

[1]Economic Geology Unit, Department of Geology, University of Buea, Buea South West Region, Cameroon
[2]Department of Geology, Federal University of Technology, Minna, Niger State, Nigeria
[3]Higher Institute of Science, Engineering and Technology, Cameroon Christian University, Bali, North West Region, Cameroon
*Corresponding author: akoagbor@futminna.edu.ng

Received July 30, 2015; Revised August 09, 2015; Accepted August 14, 2015

Abstract The meta-ultramafic rocks that are part of the Paleoproterozoic unit termed the Nyong Series in SE Cameroon were investigated in this study. The lithologic assemblage mapped is exposed on a cliff face and consists of distinguishable horizons that include least, moderately to intensely altered pyroxenite to amphibolite units. The rocks are partially to completely serpenitinized and foliated. The main mineral phases identified under the microscope include pyroxenes (clinopyroxene and orthopyroxene), olivine, hornblende, plagioclase, garnet and sulphides. The rocks depict variable alteration of the pyroxenes and other primary minerals such as olivine to actinolite, chlorite, serpentine, talc, epidote and tremolite. Electron microprobe analysis on chlorite show that the principal chlorite type ranges from talc-chlorite to penninite. Using the chlorite geothermometer it is observed that the hydrothermal alteration temperatures vary between 160-180°C. This has been overprinted by surface temperatures (20 - 40°C) during the process of weathering.

Keywords: *meta-ultramafics, intrusive, layered sequence, alteration, serpentinisation, chlorite, South East Cameroon*

Cite This Article: Ako T. A., A. Vishiti, K. I. Ateh, A. C. Kedia, and C. E. Suh, "Mineral Alteration and Chlorite Geothermometry in Platinum Group Element (PGE)- Bearing Meta-ultramafic Rocks from South East Cameroon." *Journal of Geosciences and Geomatics*, vol. 3, no. 4 (2015): 96-108. doi: 10.12691/jgg-3-4-2.

1. Introduction

Ultramafic rocks are igneous and meta-igneous rocks with <45% SiO2, >18% MgO, high FeO (>9%) and low K2O (< 1%), and they are composed of usually > 90% mafic minerals. These rocks commonly occur as large intrusions where differentiated rock types occur in layers [1]. Examples of ultramafic rocks include pyroxenite, peridotite, hornblendite, anorthosite, dunite, gabbro and norite. These rock units normally consist of plagioclase, hornblende, biotite, ortho- and clino-pyroxenes, olivine and accessory minerals such as garnet and opaque ores [2,3,4,5]. However, alteration of these minerals during metamorphism usually results in the formation of alteration products such as actinolite, tremolite, sericite, chlorite, serpentine, talc and epidote [6]. Chlorites are hydrous aluminosilicates (mica-like clay minerals) of rather complex chemical composition and structure. They are found in variety of geological environments including sedimentary, low grade metamorphic and hydrothermal altered rocks [7,8,9,10] and can either replace pre-existing minerals (generally, ferromagnesian) or precipitate directly from solution. In their structure chlorites incorporate primarily Mg, Al and Fe, and to a lesser extent Ni, Mn, Cr, V and Cu in the octahedral sheet within the 2:1 layer and in the interlayer hydroxide sheet. They form solid solutions and show variable degree of substitution. Especially, Al substitutes Si^{iv} tetrahedral sites and Mg substitutes Fe in octahedral sites and this makes chlorites chemical composition also variable [11]. The basic variations in chemical composition of chlorites are as a result of this substitutional solid-solution series between end-member compositions like clinochlore and chamosite. This wide range of chemical compositions of chlorites also results in a variety of polytpyes. These polytypes reflect the physicochemical conditions under which these chlorites formed. Paleotemperature of chlorite crystallization is of particular importance for studies dealing with metamorphism, ore deposit genesis, hydrothermal alteration or diagenesis [12-17].

Much of the classic literature dealing with chlorite composition and classification schemes is based on chlorites from metamorphic and hydrothermal environments [18,19]. Chlorites from low-temperature environments, such as those found in sedimentary rocks from diagenetic to low-grade metamorphic realms, exhibit some compositional differences compared to high-grade metamorphic or hydrothermal chlorites [20]. For example, chlorites formed from diagenetic (or sedimentary) processes tend to have higher Si contents and lower (Fe +Mg) contents than

metamorphic chlorites of similar alumina content [20, 21]. It has been proven that during the passage from diagenesis to metamorphism, chlorites apparently become less siliceous, richer in (Fe + Mg), and octahedral occupancy increases. Such a transition must be accompanied by an increase in Al^{IV} and a decrease in Al^{VI} if aluminum is to be conserved at the chlorite structure scale [21]. According to [12,13,22,23,24,25,26] these variations are related to the bulk composition of the host rock, increasing effects of metamorphism and hydrothermal alteration. These variations record the physiochemical conditions of chlorite crystallization. Accordingly, and based on the fact that chlorites are commonly found in meta-ultramafic rocks, their non-stoichiometric characteristics makes them potentially attractive geothermometer, as their compositions record invaluable information about the physicochemical conditions prevailing during their formation [11,12,27].

Meta-ultramafic rocks form part of the lithologic assemblage known as the Nyong Series in SE Cameroon that is Paleoproterozoic in age. These ultramafics have been poorly investigated although they are potential host rocks for PGE mineralization. Considering that they are poorly exposed and extensively altered, geological studies of these rocks pose many challenges. In this paper we provide an overview of a well exposed segment of the meta-ultramafic rocks in the Nyong Series with emphasis on the field occurrence and mineral alteration in a bid to understand the effects of metamorphic reactions on the mineralogy of the primary rock. Here we describe the main petrographic features and finally set constraints on the thermal gradient of alteration using chlorite geothermometry.

2. Regional Geological Setting

The Nyong Series lies within the West Central African Belt (WCAB) which is a N-S-trending Paleoproterozoic belt that extends along the western side of the Congo craton from Angola to Cameroon [28], and continues to NE Brazil as the Transamazonia belt [29,30,31,32]. The WCAB includes the Nyong complex in Cameroon [33] [Figure 1], the Franceville-Ogoue complex in Gabon and the West Congolese complex in the Republic of Congo and Democratic Republic of Congo [3,5,28,34,35].

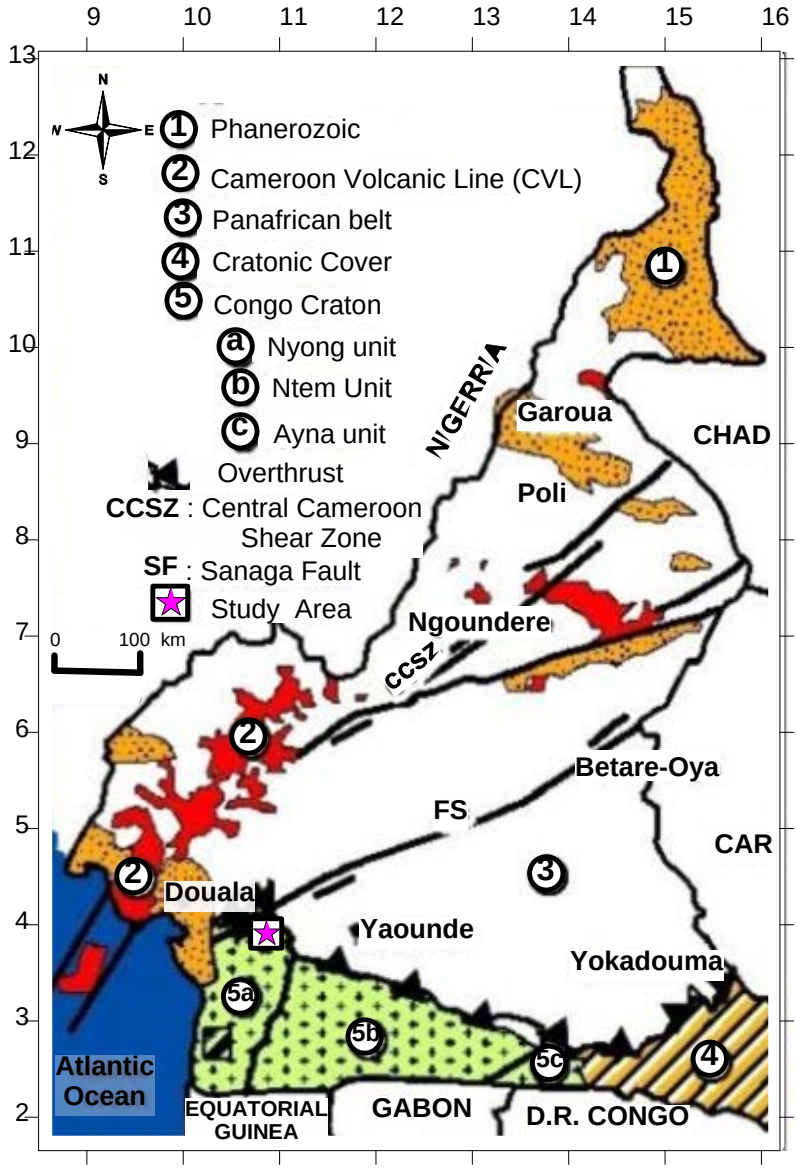

Figure 1. Geological map of Cameroon showing the study area (modified after [3])

This large belt resulted from the collision between the Congo and São Francisco cratons. Most of the WCAB is characterized by tectonic reworking of Archean crust with little addition of juvenile material, particularly in the southern part of the belt [36,37]. However, this dominant recycling character is diminished northward with the appearance of ca. 2.1 Ga juvenile metasedimentary and meta-plutonic rocks intensively reworked and dismembered in the Pan-African belt north of the Congo craton [32]. The Nyong Series (also termed Nyong Group, e.g. [29,30,31] in the northwestern corner of the Congo craton in Cameroon is a-well-preserved granulitic unit of the WCAB resting as an Eburnean nappe on the Congo Craton [37,38]. The high-grade metamorphism associated with arrested charnockite formation in this unit is dated at 2050 Ma [29,37]. However, it is not clear whether or not these Paleoproterozoic tectono-metamorphic events were accompanied by any sedimentation or magmatism. This led to the assertion that the Nyong Series is a reworked part of the Congo craton in Cameroon [30,31,38,39]. The Nyong Unit is bordered by the Ntem Unit in the SE part, the Pan-African gneiss to the north and NE and by the Quaternary sedimentary formations at the NW parts [Figure 1].

The Nyong Unit is a high grade-gneiss unit, which was initially defined as a Neoproterozoic, or a Palaeoproterozoic reactivated NW corner of the Archaean Congo Craton [29,38,39]. The unit is made up of a greenstone belt (pyroxenites, amphibolo-pyroxenites, peridotites, talcschists, amphibolites and banded iron formations), foliated series (Tonalite-Trondhjemite-Granodiorite (TTG), gneiss), and magmatic rocks (augen metadiorites, granodiorites and synites) [29]. The late magmatic rocks are represented by SW-NE-trending group of small intrusions extending from Lolodorf to Olama [3] and N-S from Lolodorf to Ngog-Tos and Eseka [Figure 2]. The Nyong unit is characterized by a regional flat-lying S1/S2 foliation associated with a variably oriented stretching lineation and local large open folds associated with N-S sinistral strike slip faults [29]. The metamorphic evolution is polycyclic with Paleaoproterozoic granulitic assemblages overprinted in the western part of the unit by Pan-African high-grade recystallizations [37]. The unit is also characterized by pre-orogenic sediments (<ca.2500 Ma) and is interpreted as an allochtnous unit thrusted on to the Congo Craton during the Eburnean-Transamazonian orogeny. This nappe tectonic event is the ultimate stage of a complete Paleaoproterozoic orogenic cycle whose major characteristics, including the suture zone, are preserved in NE Brazil [29].

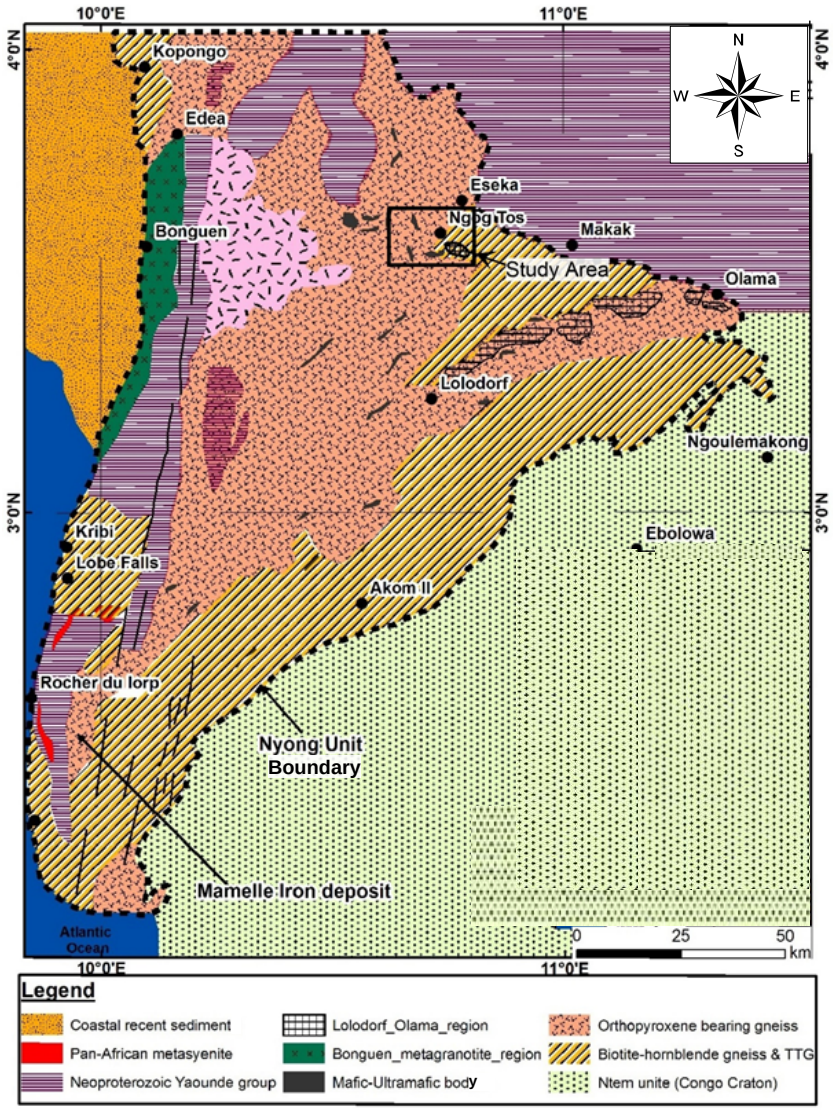

Figure 2. Geological map of the Nyong Unit showing the study location (modified after [3])

3. Materials and Methods

Ultramafic rock units within the Nyong series were systematically mapped and sampled along a layered sequence on a cliff face from the base to the top. Each horizon identified was described based on its mode of occurrence, macroscopic characteristics, structural elements and thickness. The samples collected were carefully labeled and bagged for further petrochemical studies.

Polished thin sections for petrographic studies were prepared at the Department of Geology Laboratory, University of Ghent, Belgium. The sections were examined under a petrographic Zeiss AX10 reflected and transmitted light microscope coupled with an Axioncam ERc5s digital camera at the Geology Laboratory, University of Buea paying attention to alteration and ore minerals. Samples with well developed chlorite alteration were selected for electron microprobe analysis (EMPA) of the chlorite phases. This was accomplished using a JEOL Probe JXA-8230 with five spectrometers at the Department of Geology, Federal University of Rio de Janeiro (UFRJ) Brazil. In order to achieve surface conductivity, representative polished sections were coated with carbon film prior to the EMPA analysis. The chlorite flakes were analyzed for Si, Al, Fe, Mg, Ca, Ni, Cr, K and Mn using a 1 µm beam at 15 kV accelerating voltage and 20 nA beam current with count times that vary from 10 to 20 seconds. During analysis, care was taken to select analytical points free from cracks. Details of the analytical procedure and standards employed are given in [40]). PET, LIF and TAP crystals were used to determine the minerals composition.

4. Results

4.1. Field Characteristics of the Ultramafic Rocks

The study area is made up of two distinct rock units [Figure 3]. The first is a metasedimentary unit which is represented by the talc-tremolite schists and garnet-rich micaschists with the garnet-rich micaschists being the most abundant. These rocks occur as floats of blocks with fine- to medium-grained texture. Alternating millimeter quartzo-feldspathic and ferromagnesian layers are common in the rocks. They show granoblastic microstructures and are made up of plagioclase, quartz, biotite, garnet and accessory minerals, and are believed to have been derived from metamorphism of shales, greywackes and limestones.

The second unit is meta-igneous and it is made up of amphibole-pyroxene gneiss, amphibole-garnet gneiss and biotite-garnet gneiss. The rocks here occur as domes and blocks, and are characterized by granoblastic microstructures. They are dark-grey in colour, fine- to medium-grained and show alternating millimeter to decimeter quartzo-feldspathic and ferromagnesian minerals banding. These meta-igneous rocks are composed of quartz, plagioclase, pyroxenes, hornblende and accessory minerals.

Both rock units are foliated and characterized by quartzo-feldspathic segregations or veins due to either partial melting or injection along veins or shear zones. The units have equally been intruded by magmatic rocks which are represented by a SW-NE-trending group of basic intrusions (which are the main focus of this study) [Figure 3].

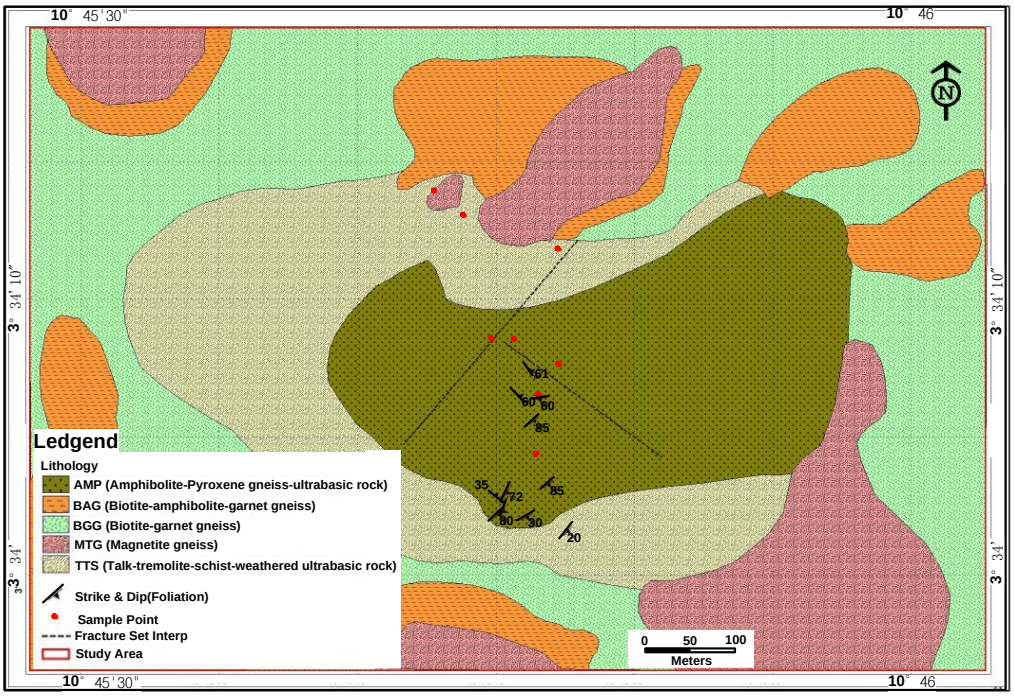

Figure 3. Geological map of the study area showing the various lithologies intruded by the ultramafic rock units

The ultramafic unit investigated is a layered sequence exposed on a 109 m cliff face. The samples in hand specimen show a variation in color from light grey to green. Along this sequence the ultramafic rocks occur as roughly circular to elliptical blocks comprising meta-pyroxenite at the base and amphibolites towards the top. The sequence therefore can be divided into two; the lower meta-pyroxenite and the upper amphibolite zones. The ultramafics rocks occur primarily as intrusions in meta-sedimentary and meta-igneous rocks and display varying

degrees of foliation. The lower pyroxenites zone is weakly foliated and it is characterized by a coarse-grained texture and consists of abundant relict olivine, plagioclase and sulphides. It is also fine- to medium-grained and has relict pyroxene, olivine and plagioclase. Towards the top pyroxene, olivine and plagioclase in these rocks have been extensively altered to serpentine, chlorite, talc and epidote. Within the amphibolitic zone the layering is on a scale of centimeters in thickness and extends laterally for only a few meters. The samples vary from least altered at the base to intensively altered at the top with relatively gentle to steep contacts. Generally, the rocks display polygonal structures and cumulus textures [Figure 4a]. The least altered samples [Figure 4b] are more massive and contain relict olivine and rare clinopyroxene and orthopyroxene as well as tremolite and chlorite whereas the intensively altered samples are less massive and more foliated with abundant tremolite, talc and chlorite and less relict olivine. Plagioclase feldspar crystals in the rocks have been preferentially weathered leaving a slightly bumpy and more mafic-rich weathered surface. This gives the rock a scapolitic texture [Figure 4c].

Structurally, the ultramafic rocks show multiple microfolds and fractures [Figure 4d and e]. The axial traces of the folds trend in the northwestern direction which is perpendicular to the general northeastern strike direction of the ultramafic exposures. The folds are asymmetric antiforms while faults with small (5-10cm) scale displacement are observed. These small-scale faults are both normal and reverse types with varying degrees of orientation and are mostly perpendicular to the general trend of the ultramafic rocks. The rocks are jointed with the joints cutting across the rock units at all levels and in all directions. The rocks are also characterized by quartzo-feldspathic segregations along veins and microshear zones [Figure 4f].

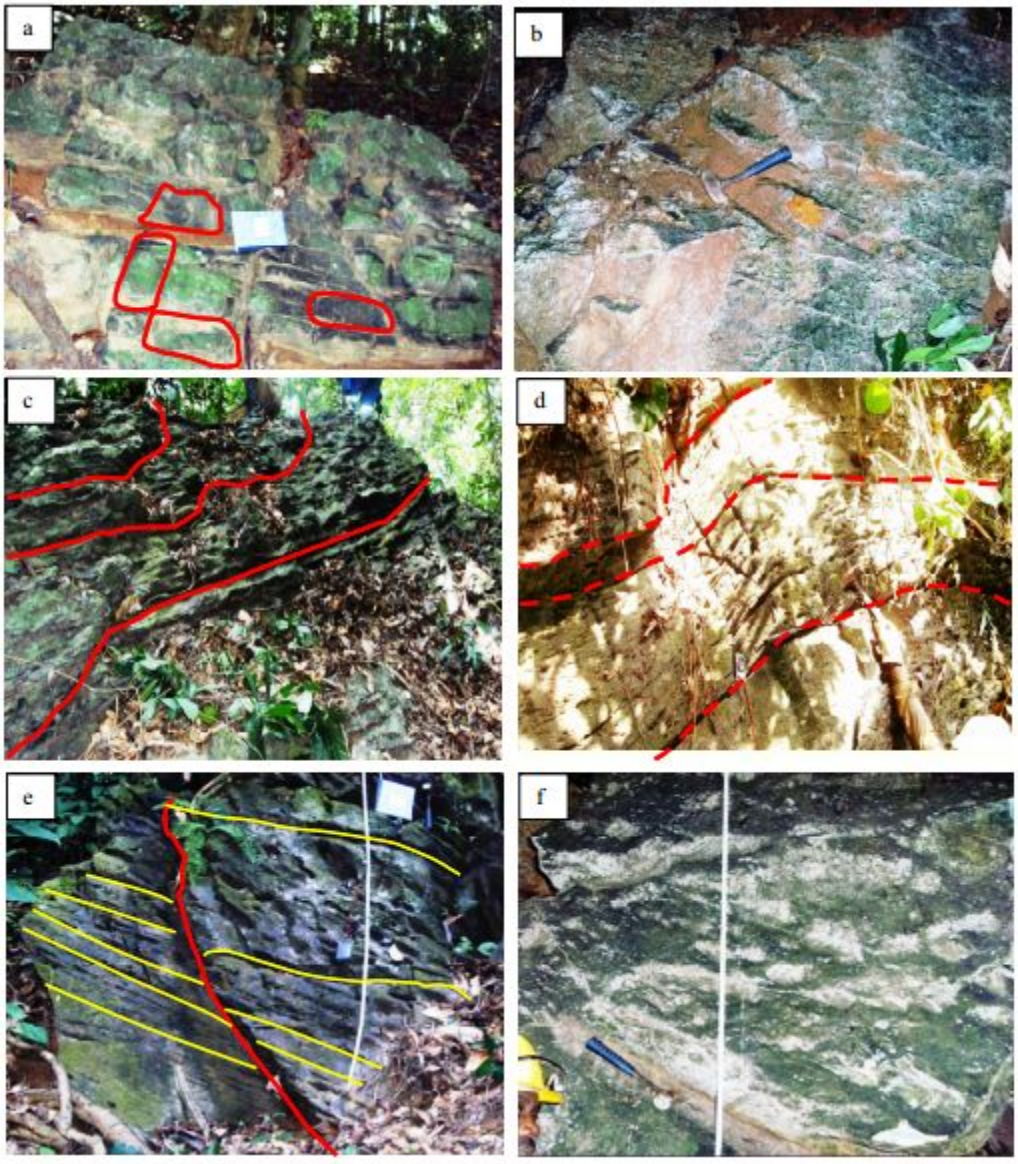

Figure 4. Field photographs of ultramafic rocks showing: (a) polygonal structures and cumulus textures, (b) massive and least altered samples, (c) slightly bumpy weathered surfaces that result in ridge and furrow scapolitic texture, (d) microfolds, (e) fractures and (f) Quartz pockets.

4.2. Petrography

Under the microscope the principal minerals identified are pyroxenes (clinopyroxene and orthopyroxene), olivine, hornblende, plagioclase, garnet, talc, epidote, tremolite, chlorite and opaque minerals. Olivine occurs as relics resulting from its partial to complete alteration to secondary mineral phases such as talc, tremolite, actinolite, epidote and chlorite.

Clinopyroxene is brown in color and makes up almost 25% of the mode [Figure 5a]. Individual crystals vary in size from 0.2 - 1.5 mm. A majority of the crystals lie within the higher limit of the range. The clinopyroxene crystals are embedded within a fine-grained matrix of orthopyroxene, amphibole and plagioclase resulting in interlocking crystal grains with well-defined grain boundaries. Some samples contain inclusions of garnet and have been partially altered to actinolite and chlorite [Figure 5b].

Orthopyroxene occupies about 15 % of the volume of the rock and occurs as stubby to acicular intergranular crystals in a matrix of plagioclase and poikilitic clinopyroxene. Most of the crystals are less than 1 mm long. The clinopyroxene and orthopyroxene crystals show wavy extinction, bent grains and twin lamellae [Figure 5a]. The orthopyroxene contains subhedral and euhedral oikocrysts of up to 1.5 mm which enclose partially altered olivine. Some of the crystals have been altered to hornblende, actinolite, chlorite and talc.

Olivine occurs as relict fragments with very high relief along its intragranular fractures. In some cases it shows serrated margins with indentations [Figure 5b]. In the least altered samples, individual crystals of olivine are crosscut by fractures filled with serpentine. Olivine is replaced by actinolite and tremolite which are also partially replaced by serpentine. This results in partial pseudomorphs of serpentine after actinolite and tremolite. Olivine is altered to serpentine and chlorite but the chlorite is located in the pressure shadows formed by the olivine clusters [Figure 5c].

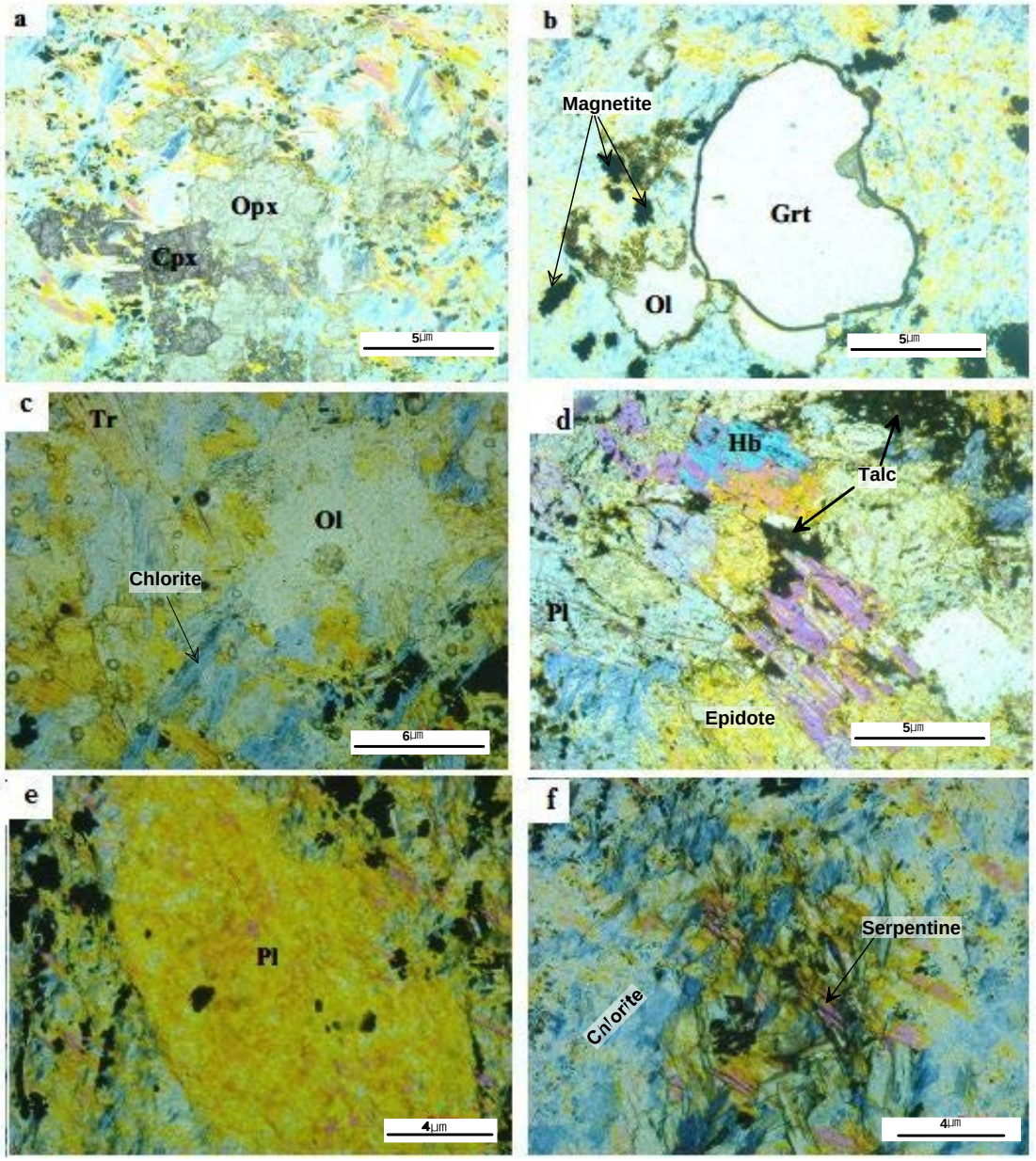

Figure 5. Photomicrographs of ultramafic rock samples showing (**a**) Clinopyroxene (cpx) crystals embedded within fine grained matrix of othopyroxene (opx) resulting in an interlocking crystal grains with well defined grain boundaries, (**b**) clinopyroxene and olivine (ol) partially altered to actinolite and chlorite with a euhedral kidney-shaped crystal of garnet (grt) inclusion with a high relief and granoblastic texture, (**c**) fine grain crystals of tremolite (tr) with a subhedral form and a prismatic habit, (**d**) prismatic crystal of hornblende (hb) showing two good directions of cleavage with complex intergrowth of crystals interwoven with tremolite, actinolite, epidote, chlorite and sulphides, (**e**) plagioclase (pl) with interlocking tabular equant grains with stubby aggregate grains of chlorite and epidote along the fracture zones of the plagioclase, (**f**) fine grained mesh of epidote, tremolite, talc and actinolite. These minerals are brightly coloured and display plumose and decussate radiating textures controlled by the cleavage planes plagioclase

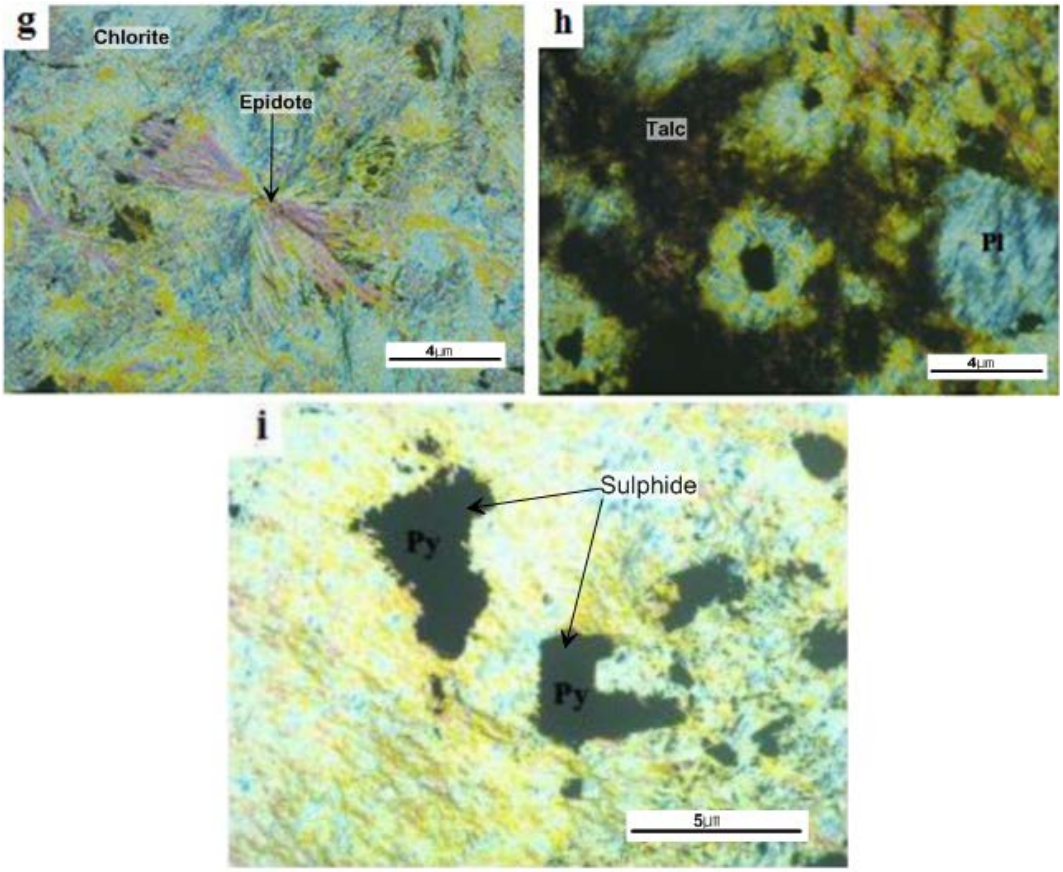

Figure 5. (**g, h**) fine grained mesh of epidote, tremolite, talc and actinolite. These minerals are brightly coloured and display plumose and decussate radiating textures controlled by the cleavage planes plagioclase, (**i**) euhedral cubic crystals of sulphide mineral with etched section. The etched edges have been occupied by chlorite and actinolite altered from the primary silicate minerals.

Hornblende occurs as prismatic crystals and shows two good directions of cleavage. The amphibole shows pleochroism from grey to blue and light yellow [Figure 5d]. Large crystals with serrated margins resulting from recrystallization are also common. The amphibole occurs as a complex intergrowth of crystals interwoven with tremolite, actinolite, epidote and sulphides. In crystals that have been formed from clinopyroxene alteration, the amphibole retains the form of the clinopyroxene and this alteration to amphibole is often restricted to the cleavage planes of the clinopyroxene.

Plagioclase occurs as interlocking tabular equant grains together with chlorite, epidote and sulphides. It is partially or completely altered to chlorite and epidote. The stubby aggregate grains of chlorite and epidote occur along the fracture zones of the plagioclase [Figure 5d and e].

Garnet occurs as euhedral and anhedral crystals with high relief. Its characteristic kidney shape is clearly displayed and its distinct outline is perfectly preserved [Figure 5b]. It shows a granoblastic texture with pyroxenes and sulfides inclusions. The crystals vary in size from < 0.2 mm to 5 mm. While the smaller crystals are anhedral and sometimes occur as inclusions in clinopyroxene, the larger ones are euhedral. Some smaller crystals however occur as rounded grains within the rock.

Epidote together with amphibole and pyrite occur as large crystals within the serpentinised ultramafic rocks. It is brightly colored with a yellow or yellowish green tint displaying a plumose texture [Figure 5f and g]. The decussate radiating texture is controlled by the cleavage planes of the plagioclase that epidote replaces.

Tremolite occurs as very fine grained colorless crystals with a subhedral form and prismatic habit. The tremolite crystals show pronounced pleochroism and twinning in some cases. In the massive ultramafic bodies, the tremolite crystals are completely unoriented resulting in a jack-straw texture. In the ultramafic rocks that have been slightly sheared with a relatively widely spaced fracture foliation, the tremolite laths have been shedded at their edges and rotated in parallelism with the foliation [Figure 5c]. Impression of rotation or “snow ball” texture are formed where the basal sections are subparallel with the plane of the thin section due to the drag of chlorite and antigorite crystals at their contacts with the larger tremolite basal sections [Figure 5c]. Tremolite has replaced olivine and in a few places shows evidence that it has replaced chlorite. In the more altered and deformed types, the tremolite laths are aligned parallel to the foliation plane, shredded and deformed in response to later shearing. This results in a phyllonitic texture. Here the larger tremolite crystals constitute the porphyroclasts in a matrix of smaller chlorite and prismatic tremolite crystals.

Chlorite occurs as faintly green coloured mineral. It is the main replacement mineral in the matrix. It generally defines foliations, fractures and veinlets as well as pressure shadows of relict olivine phenoblasts. Some of the crystals are crosscut by tremolite laths. Radiating aggregates of acicular crystals [Figure 5c and h] are also common.

Talc is another alteration mineral and generally occurs as a matrix mineral within all the samples with a more metamorphic alignment and flow banding. It is hair-like and is present as alteration product aligned along fractures and the edges of orthopyroxene crystals [Figure 5h].

The main sulphide mineral identified is pyrite [Figure 5i and Figure 6]. These sulphides generally occur as interstitial crystals (in the form of disseminations, small lenses and pods) to the silicates resulting in the formation of net-texture aggregates. The sulphide crystals are euhedral, subhedral to cubic in shape and range in size from <1mm to >1mm. Pyrite is euhedral and pseudomorph after a primary ore which can be pyrrhotite or pentlandite [Figure 5i]. Although most of the ultramafic rock has been completely serpentinised, primary crystal shapes and textures are commonly preserved. This permits the recognition of the original minerals. Mesh, lattice and bastite structures of serpentine minerals indicate derivation from olivine, pyroxenes (clinopyroxenes and orthopyroxenes), amphibole (hornblende) and plagioclase respectively. The relicts of the original minerals in the samples show that the rocks were coarse-to-medium-grained, with anhedral and subhedral mineral forms. A common feature of some of the serpentinised ultramafic rocks is a mosaic texture as a result of crystal size reduction in response to deformation. However, the relative proportions of these minerals in the metamorphosed ultramafic rocks vary considerably. In some cases, complex intergrowth relationship between the minerals and replacement textures exist between the pyroxenes and amphibole

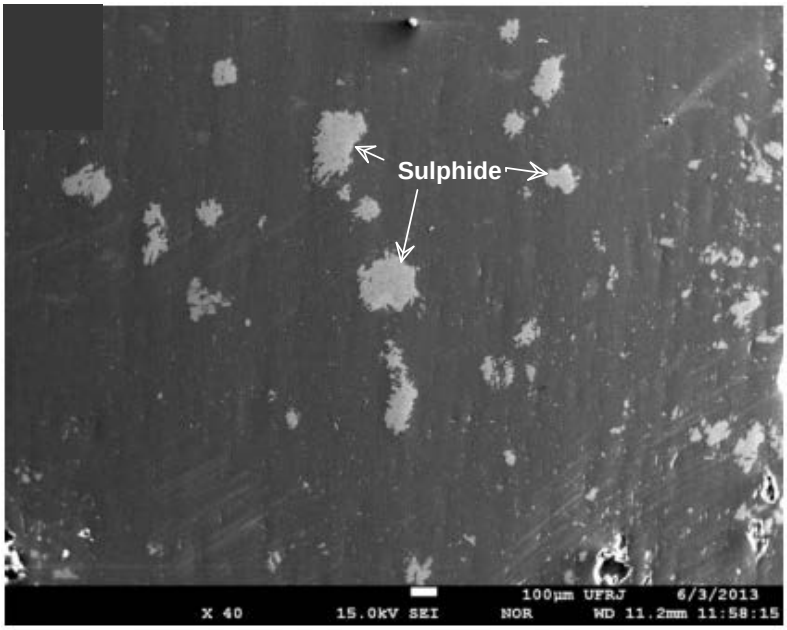

Figure 6. Backscattered scanning electron (BSE) image of sulphide (pyrite and chalcopyrite) (white crystals). The surrounding matrix is composed (probably of altered olivine-serpentine-chlorite

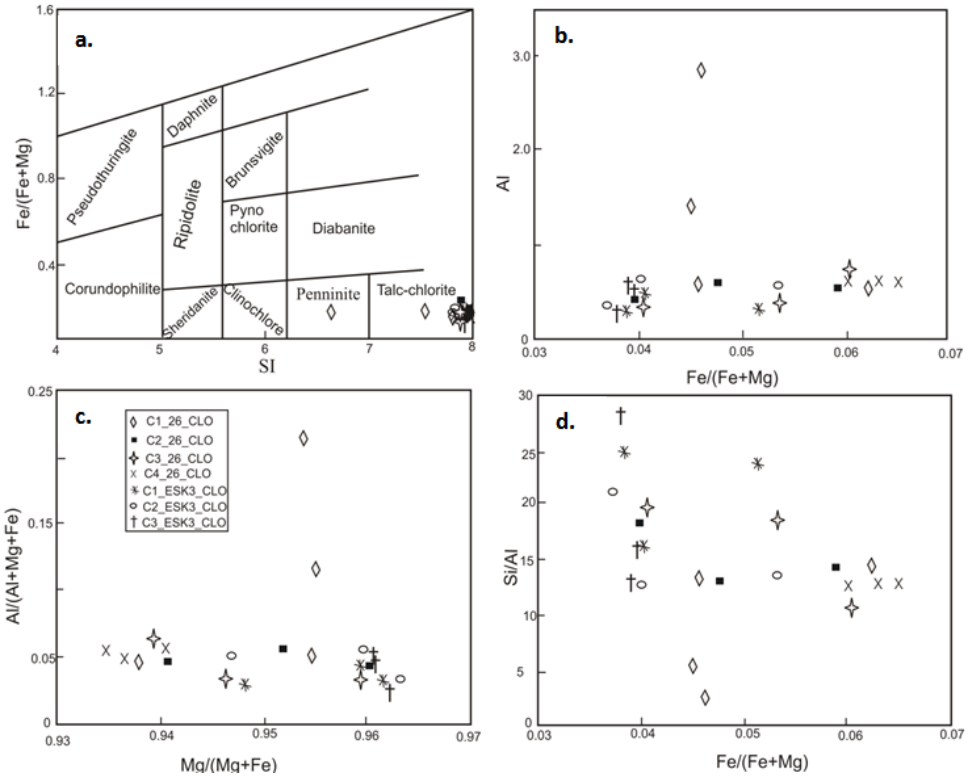

Figure 7. (a) Classification of chlorites from altered ultramafics according to [18], (b) Plot showing variation between Al/ (Al+Mg+Fe) and Mg/(Mg+Fe) ratio, (c) Al vs Fe/(Fe+Mg) and (d) Si/Al vs Fe/(Fe+Mg)

Table 1

Sample ID	1	2	3	4	5	6	7	8	9	10	11
Element (wt %)											
SiO_2	41.61	33.88	41.58	39.05	1.584	42.13	42.33	41.64	41.99	40.01	42.77
TiO_2	0.041	0.029	0.011	0.03	0.012	0.034	0.017	0.028	0.009	0.009	0.024
Al_2O_3	2.441	12.37	2.649	6.262	2.691	2.489	1.957	1.774	1.916	3.119	2.851
FeO	4.388	2.883	3.170	2.951	3.205	4.201	2.781	2.835	3.811	4.073	4.147
MnO	0.083	0.046	0.083	0.073	0.069	0.069	0.035	0.071	0.057	0.073	0.076
MgO	37.04	33.35	37.08	35.09	35.82	37.61	37.43	37.66	37.83	35.55	36.22
CaO	0.005	0.000	0.000	0.000	0.002	0.002	0.000	0.002	0.000	0.000	0.006
K_2O	0.029	0.233	0.010	0.036	0.007	0.016	0.000	0.004	0.007	0.008	0.003
Cr_2O_3	0.078	0.110	0.072	0.113	0.172	0.145	0.118	0.116	0.096	0.104	0.154
NiO_2	0.190	0.203	0.164	0.189	0.167	0.147	0.144	0.189	0.119	0.19	0.194
Total	85.90	83.12	84.82	83.79	83.73	86.84	84.82	84.31	85.84	83.15	86.45
Formula on basis of 28 oxygen											
Si	7.909	6.644	7.948	7.549	8.039	7.916	8.067	7.997	7.969	7.848	8.038
Ti	0.006	0.004	0.002	0.004	0.002	0.002	0.005	0.002	0.004	0.001	0.001
Al^{iv}	0.091	1.356	0.052	0.451	0.000	0.084	0.000	0.003	0.031	0.152	0.000
Al^{vi}	0.456	1.503	0.544	0.976	0.613	0.468	0.440	0.398	0.398	0.569	0.632
Fe	0.698	0.473	0.507	0.477	0.518	0.660	0.443	0.455	0.605	0.668	0.652
Mn	0.013	0.008	0.013	0.012	0.011	0.011	0.006	0.012	0.009	0.012	0.012
Mg	10.49	9.749	10.57	10.11	10.32	10.53	10.63	10.78	10.71	10.39	10.15
Ca	0.001	0.000	0.000	0.000	0.000	0.000	0.000	0.000	0.000	0.000	0.001
K	0.007	0.058	0.002	0.009	0.002	0.004	0.000	0.001	0.002	0.002	0.001
Cr	0.012	0.017	0.011	0.017	0.026	0.022	0.018	0.018	0.014	0.016	0.023
Ni	0.000	0.000	0.000	0.000	0.000	0.000	0.000	0.000	0.000	0.000	0.000
Total	20.28	22.72	20.28	21.08	20.19	20.29	20.09	20.12	20.19	20.43	20.19
Sum tet.	8.000	8.000	8.000	8.000	8.039	8.000	8.067	8.000	8.000	8.000	8.038
Sum oct.	11.73	11.81	11.68	11.65	11.54	11.73	11.74	11.58	11.72	11.76	11.71
Si/Al	14.46	2.324	13.32	5.291	13.11	14.36	18.35	19.91	18.59	10.89	12.73
Mg/(Mg+Fe)	0.938	0.954	0.954	0.955	0.952	0.941	0.960	0.959	0.947	0.940	0.940
Fe/(Fe+Mg)	0.062	0.046	0.046	0.045	0.048	0.059	0.040	0.041	0.053	0.060	0.060
Al/(Al+Mg+Fe)	0.047	0.219	0.051	0.119	0.054	0.047	0.038	0.035	0.037	0.061	0.055
T (^oC)[a]	27.16	161.5	23.02	65.40	17.50	26.42	17.50	17.82	20.79	33.64	17.50
T (^oC)[b]	53.11	188.9	50.52	92.96	44.81	52.69	45.54	45.81	47.57	59.77	43.63
T (^oC)[c]	32.27	165.2	26.91	69.15	21.54	31.29	20.97	21.32	25.25	38.59	22.48

Sample ID	12	13	14	15	16	17	18	19	20	21	22
Element (wt %)											
SiO_2	42.19	42.26	42.51	41.96	42.11	41.58	41.23	41.08	40.79	41.54	42.45
TiO_2	0.023	0.015	0.019	0.021	0.000	0.016	0.02	0.036	0.026	0.005	0.002
Al_2O_3	2.739	2.83	2.213	1.424	1.496	1.658	2.588	2.741	2.63	2.214	1.278
FeO	4.294	4.365	2.804	2.663	3.673	2.519	3.791	2.781	2.674	2.707	2.629
MnO	0.046	0.062	0.048	0.027	0.039	0.027	0.044	0.042	0.014	0.048	0.061
MgO	35.78	35.20	37.40	37.31	37.98	36.61	37.76	37.35	36.99	36.88	37.49
CaO	0.008	0.000	0.000	0.000	0.000	0.008	0.000	0.000	0.001	0.000	0.000
K_2O	0.001	0.008	0.000	0.007	0.017	0.011	0.008	0.015	0.009	0.008	0.000
Cr_2O_3	0.159	0.135	0.060	0.086	0.093	0.119	0.137	0.158	0.130	0.134	0.105
NiO_2	0.167	0.177	0.133	0.136	0.191	0.310	0.145	0.123	0.172	0.333	0.191
Total	85.40	85.04	85.19	83.63	85.59	82.86	85.71	84.32	83.45	83.87	84.21
Formula on basis of 28 oxygen											
Si	8.037	8.078	8.063	8.109	8.003	8.085	7.842	7.895	7.909	7.991	8.137
Ti	0.003	0.003	0.002	0.003	0.003	0.000	0.002	0.003	0.005	0.004	0.001
Al^{iv}	0.000	0.000	0.000	0.000	0.000	0.000	0.158	0.105	0.091	0.009	0.000
Al^{vi}	0.615	0.638	0.495	0.324	0.335	0.380	0.422	0.516	0.510	0.493	0.289
Fe	0.684	0.698	0.445	0.430	0.584	0.410	0.603	0.447	0.434	0.435	0.421
Mn	0.007	0.010	0.008	0.004	0.006	0.004	0.007	0.007	0.002	0.008	0.010
Mg	10.16	10.03	10.58	10.75	10.76	10.61	10.71	10.70	10.69	10.58	10.72
Ca	0.002	0.000	0.000	0.000	0.000	0.002	0.000	0.000	0.002	0.000	0.000
K	0.000	0.002	0.000	0.002	0.004	0.003	0.002	0.004	0.002	0.002	0.000
Cr	0.024	0.020	0.009	0.013	0.014	0.018	0.021	0.024	0.020	0.020	0.016
Ni	0.000	0.000	0.033	0.035	0.048	0.080	0.037	0.031	0.044	0.085	0.049
Total	20.19	20.16	20.13	19.99	20.09	19.98	20.38	20.35	20.31	20.12	19.93
Sum tet.	8.037	8.078	8.063	8.109	8.003	8.085	8.000	8.000	8.000	8.000	8.137
Sum oct.	11.52	11.54	11.44	11.57	11.55	11.75	11.51	11.79	11.73	11.62	11.50
Si/Al	13.07	12.67	16.30	25.00	23.88	21.28	13.52	12.72	13.16	15.92	28.19
Mg/(Mg+Fe)	0.940	0.935	0.960	0.961	0.949	0.963	0.947	0.960	0.961	0.960	0.962
Fe/(Fe+Mg)	0.063	0.065	0.040	0.039	0.051	0.037	0.053	0.040	0.039	0.040	0.038
Al/(Al+Mg+Fe)	0.054	0.056	0.043	0.028	0.029	0.033	0.049	0.053	0.051	0.044	0.025
T (^oC)[a]	17.50	17.50	17.50	17.50	17.50	17.50	34.28	28.65	27.16	18.46	17.50
T (^oC)[b]	43.38	43.20	45.50	45.68	44.46	45.80	61.07	56.68	55.29	46.54	45.74
T (^oC)[c]	22.67	22.83	20.99	20.85	21.82	20.76	38.70	32.11	30.54	21.89	20.81

4.3. Chlorite Chemistry and Thermometry

Analyses of chlorite flakes from altered ultramafic rocks are summarized in [Table 1]. The chlorites are generally rich in MgO averaging 36.7 a.p.f.u. Based on the structural formulae of chlorite calculated on the basis of 28 oxygens, Si ranges from 6.644 to 8.133 a.p.f.u., Al^{iv} varies between 0 and 1.356 a.p.f.u., Al^{vi} varies between 0.289 and 1.503 a.p.f.u. and the Mg^{2+} content ranges from 9.749 a.p.f.u. to 10.782 a.p.f.u as compared to Fe^{2+} whose content varies between 0.410 a.p.f.u. and 0.698 a.p.f.u. The concentrations of Ti, Mn, Ca, Na, K, Cr, and Ni are very low [Table 1]. The sum of the octahedral cations ranges from 11.44 to 11.81 [Table 1]. Based on [18] classification and nomenclature of chlorites, two compositional types have been defined penninite and Talc-chlorite [Figure 7a] with Si concentrations varying from 6.644 to 8.137 a.p.f.u. and Fe/(Fe+Mg) ratios ranging between 0.037 and 0.065 [Table 1]. The results show a slightly positive correlation between Al^{iv} and (Fe/Fe+Mg, [Figure 7b]. Chlorite composition on the Al/(Al+Mg+Fe) vs Mg/(Mg+Fe) plot [Figure 7c] reveals a small range in Mg/(Mg+Fe) ratios from 0.93 to 0.97 a.p.f.u. The concentration of Fe/(Fe+Mg) varies between 0.03 to 0.07 a.p.f.u. The chlorites show a slightly positive correlation on the Fe/(Fe+Mg) vs. Si/Al [Figure 7d].

Using the geothermometers of [13,24,41], the formation temperatures of the ubiquitous alteration mineral chlorite were calculated and are presented in [Table 1]. All three geothermometers give relatively consistent values for the individual compositions studied, although the temperatures calculated using [13] are 22-24°C higher than those of [41]. The formation temperatures of chlorite in the altered ultramafic based on [41], range from 20.8 to 165.2°C, [Table 1] with a distinct maximum in the 20-40°C interval [Figure 8].

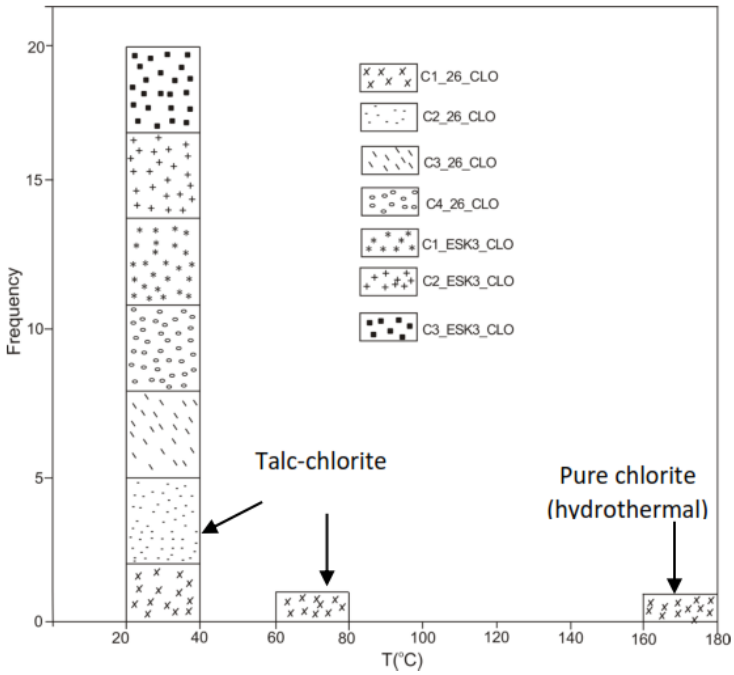

Figure 8. Frequency histogram of the calculated temperatures of based on the geothermometer of [41]. Chlorite formed at a temperature range from 20 to 180°C but most of the analytical points fall within the 20-40°C.

5. Discussion

The metamorphic mineral assemblage in the ultramafics of the Nyong series includes garnet, pyroxene, hornblende in association with serpentine and chlorite representing hydrated phases. Chlorite and tremolite occur as fine-grained symplectic intergrowth while rare relicts of olivine have jackstraw texture now preserved as plumose features defined by very fine-grained chlorite and tremolite. This assemblage defines a lower amphibolite facies metamorphism and the temperature can be constrained using the chlorite geothermometric data as discussed below. Similar metamorphic facies has been documented at the Agnew Wiluna belt in Australia [42]. At this deposit, pyrrotite is absent as it has been oxidised to magnetite, a feature also recognizable in the Nyong ultramafics.

The most important metamorphic reaction as far as the chalcophile metals are concerned would have been the serpentinisation of olivine, which would have resulted in the production of magnetite [Figure 5b and Figure 5c] as well as the generation of reducing conditions [45]. Such conditions would not have been conducive for the mobilization of Cu, nor indeed any of the chalcophile metals, even though S would have been mobilized.

The temperature of metamorphic processes in ultramafic rocks is often constrained using the composition of chlorite [42,43]. In this study talc-chlorite is the dominant chlorite type with subordinate penninite. These define a temperature high of 180°C which is lower than the 380°C temperature estimate for the breakdown of olivine to serpentine [44]. However, it is well documented that H_2O-rich fluids involved in the metamorphism of ultramafic rocks can usher this temperature down to several tens of degree as observed in this study. The intergrowth with talc is clear evidence of fluid-assisted metamorphism and can be responsible for the even much lower temperature estimates of 60-80°C. The chlorite temperature estimates of 20-40°C is attributed to weathering. In the Agnew-Wiluna belt, Ni ± PGE

mineralization at Mt. Keith, Sir Samuel, Perservserance and Six Mile [42] have similar metamorphic grades to the rocks of the Nyong series. The presence of actinolite which is a common product of retrograde metamorphism of basaltic rocks shows that the meta-ultramafic rocks did not result from a prograde metamorphism [46]. However, the presence of sulphide minerals in rocks suggests that they might have been affected by hydrothermal alteration. A sequence of mineral reactions and metasomatic exchanges which describes the evolution of these intrusive bodies from their protolith ultramafic to the extensively altered tremolite-chlorite-talc varieties in the Nyong Series can be stated based on the observed textural relationships and mineral assemblages. The ultramafic rocks of the study area correspond to the granulitic assemblages of the basaltic series and are product of metamorphism of ultrabasic igneous rocks. The sequence is suggested to begin with a peridotite with a small concentration of olivine, either fresh or already partially altered, which was tectonically emplaced into the meta-sedimentary and meta-igneous rock units as a number of layered intrusions. The reactions were retrograde hydrations of this originally high temperature-pressure assemblage in response to the lower grade environment of regional metamorphism. This resulted in a tremolite-actinolite-talc assemblage although some relict olivine, pyroxene and amphibole crystals were preserved.

A second hydration process involves the serpentinisation of olivine and tremolite, and this is evidenced by the petrographic observation that serpentine has replaced tremolite pseudomorphically and extends into fractures in the olivine [Figure 5c, f, g and h]. Thus, the crystallization of tremolite which partially replaced olivine and amphibole must have occurred at least in part before serpentinisation.

Chlorite occurs in a higher concentration in the more altered intrusive layers and could be considered to be the product of the antigorite reaction which produced additional tremolite. However, there is no textural evidence of this and the low abundance of antigorite in the least altered samples would not generate a significant amount of chlorite.

During serpentinisation the minerals in the rocks such as peridotite, dunite, gabbro and norite are converted to serpentine, magnetite and other minerals [47]. During this process olivine in these rocks undergoes several reactions to form serpentine. This reaction of the minerals in the ultramafic rocks with water is often presented as an idealized reaction such as:

$$\underset{\text{Olivine}}{(Mg,\ Fe)_2\,SiO_4} + H_2O \rightarrow \underset{\text{Serpentine}}{(Mg,\ Fe)_3\,SiO_5(OH)_4} + \underset{\text{Brucite}}{(\ Mg,\ Fe)(OH)_2} + \underset{\text{Magnetite}}{Fe_3O_4} + H_2 \quad (1)$$

This reaction represents a diverse set of processes and the true stoichiometry is greatly dependent on the parent rock composition, fluid composition, water-rock ratio, and physical conditions, especially temperature [48]. However, simplified reactions of olivine to form serpentine minerals in this study are as follows:

$$\underset{\text{Fayalite}}{3Fe_2SiO_4} + \underset{\text{Water}}{2H_2O} \rightarrow \underset{\text{Magnetite}}{2Fe_3O_4} + \underset{\text{aqueous silica}}{3SiO_2} + \underset{\text{Hydrogen}}{3H_2} \quad (2)$$

$$\underset{\text{Forsterite}}{3Mg_2SiO_4} + \underset{\text{aqueous silica}}{SiO_2} + 4H_2O \rightarrow \underset{\text{Serpentine}}{2Mg_3Si_2O_5(OH)_4} \quad (3)$$

$$\underset{\text{Forsterite}}{2Mg_2SiO_4} + \underset{\text{Water}}{3H_2O} \rightarrow \underset{\text{Serpentine}}{Mg_3Si_2O_5(OH)_4} + \underset{\text{Brucite}}{Mg(OH)_2} \quad (4)$$

Serpentinisation reactions (2) and (3) above represent silica liberation from fayalite and silica consumption by forsterite during serpentinisation, respectively. Reaction (4) represents the hydration of olivine directly to produce serpentine and brucite. A similar suite of reactions involves pyroxene-group minerals, though less readily and with complication of the additional end-products due to the wider compositions of pyroxene and pyroxene-olivine mixes. Talc and magnesian chlorite are possible products, together with the serpentine minerals antigorite, lizardite and chrysotile. It should be noted and appreciated that the equations above are a simplication of the process of serpentinisation as observed in this study. After such reactions, the poorly soluble reaction products (aqueous silica or dissolved magnesium ions) are transported in solution out of the serpentinised zone.

However, there is still controversy about what factors promote the mineralogical reactions of serpentinisation in natural ultramafic rocks. Successive changes in textures, mineral chemistry, and magnetic susceptibility during serpentinisation of peridotite involved two stages: replacement of olivine by serpentine and brucite, and subsequent formation of magnetite along with more-magnesian serpentine and brucite. The later reactions occurred concurrently with serpentinisation of orthopyroxene, which supplied the silica component [49]. These observations suggest that the silica supply from serpentinisation of orthopyroxene is also an essential factor for the formation of magnetite during serpentinisation in the Nyong Series. Magnetite formation facilitated by addition of silica has often been reported for many serpentinite systems, suggesting that the magnetite formation triggered by silica addition is one of the key reactions for the progress of serpentinisation in natural ultramafic rocks.

Serpentinisation reactions which involve the transformation of a dry peridotite to a wet serpentinite, have received great attention in the passive margin community [e.g.50]. One reason is that non-volcanic rifted margins show wide ocean-continent transitions zones of serpentinised mantle that is unroofed prior to oceanisation and seafloor spreading. Another reason is that the lower crustal bodies images taken frequently beneath volcanic passive margins might also be partially serpentinised mantle [51]. The conditions under which mantle serpentinisation occurs during passive margins formations have been explored by [52]) and [53]. The simple idea is that seawater needs to get into contact with cold (< ¬500 ^{o}C) lithospheric mantle rocks. For this to happen, crustal scale brittle faulting must take place. However, in a “normal “continental crust, the lower crust is ductile which prevents crustal scale faulting and thereby mantle serpentinisation. That notwithstanding during extension, the lower crust is “de-pressurised“ and progressively

cooled so that it eventually becomes entirely brittle. At this stage, crustal scale faulting becomes possible which then provides pathways for seawater to reach and react with cold mantle rocks to change them to serpentine. The wide range of chemical compositions of chlorites also results in a variety of polytpyes and these polytypes reflect the physicochemical conditions under which these chlorites formed. Thus Paleotemperature of chlorite crystallization is of particular importance for studies dealing with metamorphism, ore deposit genesis, hydrothermal alteration or diagenesis [14,15,16,17].

5. Conclusion

The ultramafic rocks of the Nyong Series have been altered and metamorphosed. The presence of sulphide minerals in the rocks suggests that they might have been affected by hydrothermal alteration marking a late sulphidation event. This hydrothermal event is deciphered from the temperature range of 160-180°C derived from the stoichiometry of pure chlorite. The olivine and pyroxenes in the samples have altered to fine-grained secondary hydrous silicates such as tremolite, actinolite and serpentine. The presence of these secondary hydrous silicates suggests that if PGE mineralization is present, it is the product of dissolution and redeposition during hydrothermal alteration. However, most of the chlorites formed at temperature ranges of 20-40°C and 60-80°C respectively, indicating talc-chlorite which reflects weathering-related alteration.

Serpentinisation of olivine, which resulted in the production of magnetite, is the most important metamorphic reaction that occurred in the samples. The presence of actinolite and amphibole which are common products of retrograde metamorphism of basaltic rocks shows that the ultramafic rocks did not result from a prograde metamorphism process. The change in texture of the rocks from coarse-grained to fine-grained, and appearance of diverse mineralogy (silicates, sulphides and oxides) subsequent to the olivine crystallization/fractionation, is an important event in the ultramafic rocks in the Nyong Series.

Acknowledgements

This article is part of the PhD thesis of ATA underway at the University of Buea and completed within the research framework of economic geology on the Precambrian Mineral belt of Cameroon supported by University of Buea Faculty Grants to CES. ATA is grateful for study leave from the University of Minna, Nigeria. CES further acknowledges funding from the AvH Stiftung, Germany and the support of Prof. J. Mendes with the EMPA work. We are grateful for the thoughtful comments of an anonymous reviewer that improved on the text.

References

[1] Ballhaus, C and Ryan, C, G. Platinum-group elements in the Merenskey Reef. 1. PGE in base metal sulfides and the down-temperature equilibrium history of Merensky ores: Contribution to Mineralogy and Petrology, 122 (3), 241-251, 1995.

[2] Barnes, S. J., Fiorentini, M. L. and Fardon, M. C. Platinum group element and nickel sulphide ore tenors of the Mount Keith nickel deposit, Yilgarn Craton, Australia. Mineralium Deposita, 47, 129-150, 2012.

[3] Ebah Abeng, A. S., Ndjigui, P-D., Beyanu, A. A., Tessontsap, T. and Bilong, P. Geochemistry of pyroxenites, amphibolites and their weathered products in the Nyong unit, SW Cameroon (NW border of Congo Craton): Implications for Au-PGE exploration. Journal of Geochemical Exploration, 114, 1-19, 2012.

[4] Holwell, D. A., Abraham-James, T., Keays, R. R. and Boyce, A. J. The nature and genesis of marginal Cu-PGE-Au sulphide mineralization in Paleogene Macrodykes of the Kangerlussuaq region, East Greenland. Mineralium Deposita, 47, 3-21, 2012.

[5] Ndema Mbongue, J. L., Ngnotue, T., Ngo Nlend, C. D., Nzenti, J. P. and Cheo Suh, E. Origin and Evolution of the Formation of the Cameroon Nyong Series in the Western Border of the Congo Craton. Journal of Geosciences and Geomatics, 2, (2) 62- 75, 2014.

[6] Tracy, R. J., Robinson, P. and Wolft, R. A. Metamorphosed ultramafic rocks in the Bronson Hill anticlinorium, Central Massachusetts.American Journal of Science, 284, 530-558, 1984.

[7] Jiang, W. T., Peacor, D. R. and Buseck , P. R. Chlorite geothermometry? – Contamination and apparent octahedral vacancies. Clays and Clay Minerals, 42, (5), 593-605, 1994.

[8] Deer, W. A., Howie, R. A. and Zussman, J. An Introduction to the Rock Forming Minerals. Longman, London, 528pp, 1966.

[9] Gemmell, J. B. and Herrmann, W. A special Issue on Alteration associated with volcanic-hosted massive sulfide deposits, and its exploration significance. Economic Geology, 96, (5) 909-912, 2001.

[10] Gifkins, C. C. and Allen, R. L. Textural and chemical characteristics of diagnostic and hydrothermal alteration in glassy volcanic rocks: Examples from the Mount Read Volcanics, Tasmania. Economic Geology, 96, 973-1002, 2001.

[11] Wiewióra, A .and Weiss, Z. Crystallochemical classifications of phyllosilicates based on the unified system of projection of chemical composition:11.The chlorite group. Clay Minerals 25, 83-92, 1990.

[12] De Caritat, P., Hutcheon, I. and Walshe, J. L. Chlorite Geothermometry: A Review. Clays and clay minerals, 41, No.2, 219-239, 1993.

[13] Zang, W, and Fyfe, W. S. Chloritization of the hydrothermally altered bedrock at the Igarapé Bahia gold deposit, Carajás, Brazil. Mineralium Deposita, 30, 30-38, 1995.

[14] Vidal, O., Parra, T. and Trotet, F. A thermodynamic model for Fe-Mg aluminous chlorite using data fromphase equilibrium experiments and natural politic assemblages in the 100° to 600°C, 1 to 25 kb range. American Journal of Science, 301,557-592, 2001.

[15] Klein E.L., Harris,C., Giret, A., and Moura ,C.A.V.The Cipoeiro gold deposit, Gurupi Belt, Brazil: Geology,chlorite geochemistry, and stable isotope study. Journal of South American Earth Sciences, 23 , 242-255 2007

[16] ohier, B. A, Akawy, A. and Hassan, I. Role offluid mixing and wallrock sulfidation in gold mineralization at the Semnamine area, central Eastern Desert of Egypt: Evidence from hydrothermal alteration,fluid inclusions and stable isotope data. Ore Geology Reviews, 34, 580-596, 2008.

[17] Zohier, B. A.Microchemistry and stable isotope systematics of gold mineralization in a Gabbro-diorite complex, SE Egypt. Microchemical Journal, 103, 148-157, 2012.

[18] Hey, M. H. A new review of chlorites. The mineralogy magazine and journal of the mineralogical society, 30, (224) 278-292, 1954.

[19] Foster, M. D. Interpretation of the composition and classification of the chlorites. US Geological Survey Professional Paper 414A, 27pp, 1962.

[20] Curtis, C. D., Hughes, C. R. Whiteman, J. A. and Whittle, C. K. Compositional variation within some sedimentary chlorites and some comments on their origin. Mineralogical Magazine, 49, 375-386, 1985.

[21] Hillier, S. and Velde, B. Octohedral occupancy and the chemical composition of diagenetic (low-temperature) chlorites: Clay Minerals, 26, 146-168, 1991.

[22] Cathelineau, M. Cation site occupancy in the chlorites and illites as a function of temperature: Clay Minerals, (23), 471-485.

[23] Schiffmann, P. and Fridleifsson, G. O. The smectite to chlorite transition in drillhole NJ-15, Nesjavellir Geothermal Field, Iceland:

XRD, BSE, and electron microprobe investigation: Journal of Metamorphic Geology, 9, 679-696, 1991.

[24] Cathelineau, M. and Nieva, D. A chlorite solid solution geothermometer: The Los Azufres (Mexico) geothermal system. Contributions to Mineralogy and Petrology, 91, 235-244, 1995.

[25] Xie, X., Byerly, G. R., Ferrell Jr, R. E. IIb trioctahedral chlorite from the Barberton greenstone belt: crystal structure and rock compositional constraints with implications to geothermometry. Contributions to Mineralogy and Petrology, 126, 275-291, 1997.

[26] Klein, E. L. and Koppe, J. C. Chlorite geothermometry and physical conditions of mineralization in the Paleoproterozoic Caxias deposit, São Luis Craton, Northern Brazil. Geochimica Brasiliensis, 14(2), 219-232, 2000.

[27] Frimmel, H. E. Chlorite thermometry in the Witwaterstrand Basin: Constraints on the Paleopaleoterozoic geotherm in the Kaapvaal Craton, South Africa. Journal of Geology, 105, 601-615, 1997.

[28] Feybesse, J. L., Barbosa, J., Ledru, P., Guerrot, C., Jahan, V, Trboulet, V., Bouchot, V., Prian, J. P. and Sabaté, P. Paleoproterozoic tectonic regime and makers of the Archaean/proterozoic boundary in the Congo-São Francisco craton. EUG 8, Terra abstracts, 100, 1998.

[29] Lerouge, C., Cocherie, A., Toteu, S. F., Penaye, J., Mile'si. J., Tchameni. R., Nsifa, E. N. Fanning, C. M. and Deloule, E. Shrimp U-Pb Zircon age for Paleoproterozoic sedimentation and 2.05Ga syntectonic plutonism in the Nyong Group, South-Western Cameroon: consequences for the Eburnean –Transamazonian belt of NE Brazil and Central Africa. Journal of African Earth Sciences, 44, (4-5) 413-427, 2006.

[30] Owona, S. Archaean, Eburnean and Pan-African Features and Relationships in their Junction Zone in the South of Yaounde (Cameroon). Unpublished Ph.D. Thesis, University of Douala, Cameroon, 232pp, 2008.

[31] Owona, S., Schulz, B., Ratschbacher, L., Ondoa, J. M., Ekodeck, G. E., Tchoua, F. M. and Affaton, P. Pan-African Metamorphism evolution in the southern Yaoundé Group (Qubannguide Complex, Cameroon) as revealed by EMP-Monazite dating and thermobarometry of garnet metapelites. Journal of African Earth Sciences, 59, 125-139, 2011.

[32] Pénaye, J., Toteu, S. F., Tchameni, R., Van Schmus, W. R., Tchakounté, J., Ganwa, A., Minyem, D. and Nsifa, E. N. The 2.1 Ga West Central African Belt in Cameroon: extension and evolution. Journal of African Earth Sciences39, 159- 164, 2004.

[33] Maurizot, P., Abessolo, A., Feybesse, A., Johan, V. and Lecomte, P. Etude et prospection minière du sud-Ouest Cameroon. Sythèse des travaux de 1978 á 1995. 85-CMR 066 BRGM, 1986.

[34] Bonhomme, M. G., Gauthier-Lafaye, F. and Weber, F. An example of Lower Proteroizoic sediments: the Francevillian in Gabon. Precambrian Research,18, 87-102, 1982.

[35] Vicat, J. P. and Pouclet, A. Paleo- and Neoproterozoic granitoids and rhyolites from the West Congolian Belt (Gabon, Congo, Cabinda, north Angola): Chemical composition and geotectonic implications. Journal of African Earth Sciences.31,(3 and 4) 597-617, 2000.

[36] Thomas, R. J., Chevallier, L. P., Gresse, P., Harmer, R. E., Eglington, B. M., Armstrong, R. A., DeBeer, C. H., Martini, J. E. J., de Kock, G. S., Macey, P. H. and Ingraham, B. A. Precambrian evolution of the Sirwa Window, Anti-Atlas Orogen, Morocco. Precambrian Research, 118, 1-57, 2002.

[37] Toteu, S. F., Pénaye, J., Van Schmus, W. R. and Michard, A. Preliminary U-PB and Sm-Nd geochronologic data on the North Central Cameroon: Contribution of the Archaean and Paleoproterozoic crust to the edification of an active domain of the Pan-African orogeny. C. R. Acad. Sci. Paris, 319, Series II, 1519 - 1524, 1994a.

[38] Feybesse, J. L., Johan, V., Maurizot, P. and Abessol, A. Evolution tectono-métamorphique libérenne et éburnéenne á la partie NW du craton zaïṛois (SW Cameroon). Current Research In Africa. Earth Sci., Matheis and Schandelmeier (eds) Balkema, Rotterdam: 9-12, 1986.

[39] Lasserre, M. and Soba, D. Age libérien de granodiorites et des gneiss à pyroxene du Cameroon méridional. Bull. B.R.G.M. 2è série, sectionIV, I, 17-32, 1976.

[40] Mendes J. C. and De Campos C. M. P. Norite and charnockites from the Venda Nova Pluton, SE Brazil: Intensive parameters and some petrogenic constraints. Geoscience frontiers 1(6), 1-12, 2012.

[41] Kranidiotis, P., MacLean, W.H. Systematics of chlorite alteration at the Phelps Dodge massive sulphide deposit, Matagami,Quebec. Economic Geology 82, 1898-1911,1987.

[42] Gole, J. M. Leaching of S, Cu, and Fe from disseminated Ni-(Fe)-(Cu) Sulphide ore during serpentinization of duinite host rocks at Mount Keith, Agnew- Wiluna belt Western Austrailia . Mineralium Deposita, 49, 821-842, 2014.

[43] Bourdelle, F., Parra, T.,Chopin, C. and Beyssac, O. A new chlorite geothermometer for diagnostic low-grade metamorphic conditions. Contribution to Mineralogy and Petrology, 165, 723-735, 2013.

[44] Fruh-Green, G. L., Connolly J. A. D. and Plus, A. Serpentinisation of oceanic Peridotites: Implication for geochemical cycles and biological activity. American Geophysics Union, Monograph 203, 1-29, 2014.

[45] Eckstrand, O. R. The Dumont Serpentinite: A model for control of Nickel, ferrous opaque mineral assemblages by alteration reactions in ultramafic rocks. Economic Geology, 70, 183-201, 1975.

[46] Winter, J. (2001). An Introduction to Igneous and Metamorphic Petrology. Prentice Hall, New Jersey.

[47] Bowles, J. F. W., Prichard, H. M., Suarez, S. and Fisher, P. C. The first report of platinum-group minerals in magnetite-bearing gabbro, Freetown layered complex, Sierra Leone: Occurrences and genesis. The Canadian Mineralogist, 51(3), 455-473, 2013.

[48] Frost B. R. and Beard, J. S. On silica activity and serpentinisation. Journal of Petrology, 48, 1351-1368, 2007.

[49] Akane, M., Tetsu, K., Naoto I. and Kenji, M. Role of Silica for the Progress of Serpentinization Reactions: Constraints from successive changes in mineralogical textures of Serpentinites from Iwanaidake Ultramafic body, Japan. Mineralogical Society of America, 99, (5-6), 1035-1044, 2014.

[50] Skelton, A. R., Whitmarsh, F. A., Crill, P. and Koyi, H. Constraining the rate and extent of mantle serpentinization from seismic and petrological data: implications for chemosynthesis and tectonic processes: Geofluids, 5, 153-164, 2005.

[51] Lundin, E. R. and Dore, A.G. Hyperextension, serpentinization, and weakening: A new paradigm for rifted margin compressional deformation: Geology, 39, 347-350, 2011.

[52] Perez-Gussinye, M., Morgan, J., Reston, J. T. and Ranero, C. The rift to drift transition at non-volcanic margins: Insights from numerical modeling. Earth and Planetary Science Letters, 244, 458-473, 2006.

[53] Perez-Gussinye, M. and Reston, T. J. Rheological evolution during extension at nonvolcanic rifted margins: On set of serpentinisation and development of detachments leading to continental breakup: Journal of Geophysical Research-Solid Earth, 106, 3961-3975, 2011.